Journal of Bioremediation & Biodegradation

Li, et al., J Bioremed Biodeg 2014, 5:3
http://dx.doi.org/10.4172/2155-6199.1000220

Research Article Open Access

New Insights into Microbes in the Midgut of Termite *Coptotermes formosanus*

Tingting Li, Jijiao Zeng, Deepak Singh and Shulin Chen*

Department of Biological Systems Engineering, Washington State University, Pullman WA, 99164, USA

***Corresponding author:** Shulin Chen, Department of Biological Systems Engineering, Washington State University, Pullman, WA 99164-6120, USA, Tel: 509-335-3743; Fax: 509-335-2722; E-mail: chens@wsu.edu

Rec date: Feb 21, 2014, **Acc date:** Apr 23, 2014, **Pub date:** Apr 28, 2014

Abstract

Wood-feeding termites have evolved unique capability to effectively digest lignocellulosic material, using it for both energy and nutrition. This ability depends mainly on the mutualistic interaction between symbiotic gut microbiota and the termite itself. This study investigated microorganisms in the midgut of termite *Coptotermes formosanus*, a segment that has been less studied than the hindgut. Fluorescence in situ hybridization (FISH) was initially used to visualize and identify individual bacteria and archaea in the termite's midgut. After isolation of microorganisms with six different media, preliminary screening was carried out on plates by testing the capability to oxidize guaiacol as well as decolorize the dye azure B. Two selected strains; B207 and L201 were identified as *Streptomyces sp*. through 16S rRNA gene sequence analysis. Submerged state fermentation of the strains with softwood biomass as substrate was further performed. The analysis results of attenuated total reflectance fourier transform infrared (ATR-FTIR), chromatography/mass spectrometry (GC/MS) and pyrolysis-gas chromatography/mass spectrometry (Py-GC/MS) indicated that streptomyces strains B207 and L201 have certain lignocellulose decomposition capabilities.

Keywords: Termite; Lignocellulose; *Streptomyces*; FISH; Py-GC/MS; GC/MS

Introduction

Lignocellulose, the major component of plant cell walls, is the most abundant and sustainable biomass on the earth, and is recognized for its potential for renewable energy production [1,2]. Its structural complexity, however, prevents accessibility of enzymes to hydrolyze its large carbohydrate polymers to be used as substrate for the production of fuel through fermentation [3,4]. It is generally accepted that lignocellulose is mainly composed of β-1,4-linked sugar polymer cellulose surrounded by hemicellulose, which is in turn, covalently linked at various points with lignin by ester bonds to form a matrix [5]. Unlike highly ordered cellulose, lignin is an amorphous, polyphenolic material consisting of mainly three phenylpropanoid monomers: coniferyl (G), sinapyl (S), and *para*-coumaryl (H) alcohol [6]. The lignin structure forms a barrier to protect cellulose from enzyme attack thus largely contributes to the recalcitrance of lignocellulosic biomass [7]. Various physico-chemical processes can degrade and/or modify lignin to increase enzymatic digestibility of lignocellulosic biomass [8-10] through pretreatment of the biomass. Although effective, these methods are often accompanied by issues such as low selectivity, high cost, and environmental concerns related to industrial applications. For example, oxidative pretreatment processes are typically non-selective therefore losses of hemicellulose and cellulose can occur. Hot water, acid hydrolysis, and alkaline hydrolysis are energy or capital-intensive. Furthermore, chemicals required in the process must be recycled in order to reduce the cost and protect the environment. Therefore, it is desirable to develop highly efficient, economic pretreatment technology to facilitate enzyme hydrolysis of cellulose and hemicelluloses into fermentable sugar.

Biological processes have been recognized as one of the alternative pretreatment technologies. It is well known that natural microorganisms such as white [11,12] and brown-rot fungi [13], secrete complex enzyme systems to degrade lignocelluloses under ambient conditions. For example, Singh et al. [14] found that *P. chrysosporium* expressed lignin peroxidase and manganese peroxidase at an early growth stage during their growth on wheat straw. The fungus-treated wheat straw had higher S/G ratios [14] and less energy demand for thermal degradation [15]. Another major advantage of biological process is that the enzyme system has selectivity for lignin removal. Understanding of this biological process would provide critical insights into development of new technology for biomass pretreatment and hydrolysis.

Another group of extremely effective wood-degrading organisms is termites. Termites can degrade 65-99% of wood-cellulose and hemicelluloses, as well as 5-83% of the lignin within 24 hours under natural conditions [16-19]. Apparently, the termites have unique facilities to handle lignin-carbohydrate complexes efficiently. A variety of lignocellulolytic enzymes were found in the termite system [20-22]. Despite their small body size, termites harbor an abundant and astonishingly diverse intestinal microbiota, which is one of the most fascinating examples of symbiosis among microbes, and between an animal and microbes [23]. It is widely accepted that lignocellulose digestion in termites is intimately correlated with both host and a highly specific flora of symbiotic microbes [2,5,24-26]. Much work has been performed to understand the exact roles of the host and symbiotic microbiota in the complex processes of lignocellulose degradation and conversion. Warnecke et al. [27] confirmed important symbiotic functions in termite hindgut through metagenomic and functional analysis on carbohydrate hydrolysis, H_2 metabolism, CO_2-reductive acetogenesis and N_2 fixation [27]. Through termite digestome analysis, Tartar et al. (2009) found that in the gut of the lower termite *Reticulitermes flavipes*, there existed an apparent three-way collaboration among termite, protist and

prokaryotic symbionts involving several cellulase, hemicellulase, phenoloxidase and peroxidase genes for lignin degradation/ depolymerization [2,28].

Various evidences suggest that lignin structure was modified in termites and that the modification process begins in the foregut and continues in the midgut [2,17,27,29]. However, the source of the enzymes or chemicals responsible for this modification still need further research. It is believed that the enzymes from the host largely contribute to the digestive process of lignin. Coy et al. [30] provided evidence that lactases in the gut of *Reticulitermes flavipes* were produced in the salivary gland, secreted into the foregut and capable of modifying soluble lignin [30]. Compared to the hindgut segment, few reports have addressed the composition and function of the microbes present before the hindgut, except for the mixed segment, present only in higher termites, where it is situated between the midgut and the first proctodeal segment [31]. The lower termite gut is even considered absent occurring of intestinal microbiota in the segments before the hindgut. This lack of information prevents a comprehensive understanding of the symbiosis between gut bacteria and their termite host regarding lignin degradation.

We report in this paper a study using culture and culture-independent approaches on the midgut microbe ecosystem. Fluorescence in situ hybridization (FISH) technique in association with confocal laser scanning microscopy (CLSM) was used to define the microbial communities and display the distribution and diversity of microbial flora in the termite midgut. Two isolates from the termite midgut were identified as the *Streptomyces* genus by 16S rRNA and named B207 and L201. Their functionality on softwood was determined by Fourier transform infrared spectroscopy (ATR-FTIR), gas chromatography/mass spectrometry (GC/MS) and pyrolysis-gas chromatography/mass spectrometry (Py-GC/MS). The results of this study indicated that the existing microbial community in the termite midgut could have important roles in lignocellulose decomposition.

Materials and Methods

Materials

Termites, *Coptotermes formosanus*, were collected in Poplarville, Mississippi, USA and maintained in plastic boxes (49×36×32) in a dark chamber at 28°C with 90% humidity. These organisms were fed on 6.8×1.5×0.5 inches of Southern pine (Pinus australis F. Michx) blocks, the lignin of which consists almost exclusively of guaiacyl propane subunits. The surface of the *C. formosanus* workers was sterilized twice with 70% ethanol and briefly rinsed in sterilized distilled water. The abdomen was opened under a dissection microscope, and the digestive tract was carefully extracted with fine-tipped sterile forceps. The midgut tracts were isolated and directly transferred to Carnoy's solution (ethanol-chloroform-acetic acid, 6:3:1) for FISH [**32**], and to a 1.5-ml microtube containing 0.5 ml TYE media (1% tryptone and 0.5% yeast extract) for microbe isolation [**33**], respectively.

Histology

After overnight fixation in Carnoy's solution, the tissues were dehydrated using an ethanol-xylene series and embedded in paraffin. Serial tissue sections (thickness, 3 μm) were cut with a rotary microtome and mounted on positive-charged slides. The sections were dewaxed using 4×SSC solution at 80°C, and dehydrated through an ethanol series, and air dried prior to in situ hybridization [32].

In situ hybridization

The probe EUB 338 (5'-GCTGCCTCCCGTAGGAGT-3') and ARC 915 (5'-GTGCTCCCCCGCCAATTCCT-3') [33] were labeled with fluorescein isothiocyanate (FITC, extinction wavelength, 495 nm; emission wavelength, 520 nm) and tetramethyl rhodamine 5-isothiocyanate (TRITC, extinction wavelength, 550 nm; emission wavelength, 570 nm) (Invitrogen, US), respectively. A total of 200 μl of hybridization buffer (20 mM Tris-HCl [pH 8.0], 0.9 M NaCl, 0.01% sodium dodecyl sulfate, and 30% formamide) containing 50 pmol of the labeled probe was carefully applied onto the microscopic section of a glass slide. A large coverslip was placed on the microscope slide and carefully pressed until the hybridization solution was evenly distributed over the respective section whereby a space of ~0.5 mm was allowed between the slide and the surface of the section. The microscope slides were then transferred horizontally into the humidified hybridization chamber and incubated at room temperature overnight. To eliminate nonspecifically bound probe, the slides were washed three times in a wash bath with 1×TBS buffer (20 mM Tris-HCl [pH 7.4], 0.15 M NaCl) for 15 min. After washing, the slides were air dried and subsequently treated with mounting medium, covered with a coverslip, and sealed with nail polish. The fluorescent signals were observed with a confocal laser scanning microscope (CLSM; Carl Zeiss, Germany).

Isolation and screening of microorganisms

Termites were dissected as previously described. The midgut tracts were pooled in a 1.5-ml micro-centrifuge tube containing 0.5 ml TYE media (1% Tryptone and 0.5% yeast extract) and disrupted aseptically. After serial dilution, 100 μl of the serial dilutions were spread onto four different agar media plates: PDA plates (3.9% potato dextrose agar), LB plates (2.5% Luria-Bertani media and 1.5% agar), Bennett's plates (1.0% glucose, 0.1% yeast extract, 0.2% peptone, 0.1% beef extract, and 1.5% agar), and Nutrient plates (0.3% beef extract, 0.5% peptone, 1.5% agar). The plates were incubated for several days at 28°C until colonies were visible [34]. Colonies were streaked on the same agar plate until a single isolated colony was obtained. To detect a microbe that had the ability for producing ligninolytic enzymes, screening was carried out through guaiacol oxidation and dye decolorization in Petri dishes (90 mm diameter) with 14 ml of PDA. The indicator compounds guaiacol (0.01%, w/v) (Sigma) and azure B (0.01%, w/v) (Sigma) were added to the media; guaiacol was added before autoclaving, while azure B was added after autoclaving as a sterile-filtered water solution. Due to their lack of substrate specificity, lignin-modifying enzymes are capable of degrading a wide range of xenobiotics. Guaiacol is commonly used as an indicator of ligninolytic enzymes [35], and can be converted into a reddish-brown oxidized compound. Similarly, the dye azure B can be employed to determine lignin peroxidases [36], which actually turned out to be much more advantageous [37]. The positive chemical reactions were observed by a colorless halo around the microbial growth [38]. Termite digestive tracts (ground aseptically) were inoculated in different agar plates at 28°C under aerobic conditions. After 4 weeks, 100 isolated strains were obtained and applied to a screening process in order to evaluate their aromatic-degrading ability.

16S rRNA identification of the isolated microorganisms

Candidate strains were routinely cultured on yeast extract-malt extract glucose (YEMEG) agar [39]. After culture, spores were suspended in sterile distilled water, followed by genome extraction using the Ultra Clean Microbial DNA isolation kit (Mo Bio, USA) according to the manufacturer's instructions. A 1.5 kb segment of the bacterial 16S rRNA gene was amplified by using primers 27f (5'-AGAGTTTGATCMTGGCTCAG-3') and 1492r (5'-TACGGYTACCTTGTTACGATTT-3'). PCR reactions were conducted by using GoTaq Green Master Mix (Promega, USA) with a temperature profile of 95°C for 3 min, followed by 30 cycles of 95°C for 45 s, 55°C for 30 s, and 72°C for 1.5 min. The amplicons were visualized in 1% agarose gel containing ethidum bromide at a concentration of 0.5 µg/ml and were cleaned and recovered from the gel by using QIAquick Gel Extraction Kit (QIAGEN, USA) according to the manufacturer's recommendations. The purified fragments were then cloned into the pGEM® -T Easy Vector (Promega, USA). Ligation products were transferred into competent cells of *Escherichia coli* TOP10. White colonies were randomly picked and screened directly for inserts by performing rapid plasmid tests using blue colonies as negative control. Plasmid DNA was prepared from the clones with the QIAprep spin miniprep kit (Qiangen, Crawley, UK). Plasmid DNA was then sequenced and compared with those in the Nr/nt database by using the Basic Local Alignment Search Tool (BLAST) algorithm [40].

Growth on Lignocelluloses

Sporulation of strains B207 and L201 maintained at 4°C was done at 37°C on YEMEG agar for 2 weeks. A spore suspension was obtained by suspending the spores from an agar plate culture into 10 ml sterile distilled water containing 0.1% (wt/vol) Tween 80 and used as the initial inoculum. 250-ml shake flakes containing 50 ml of basal salts medium (BSM) [39] supplemented with 0.6 % (wt/vol) yeast extract and 1.0% (wt/vol) 40-mesh pine wood were inoculated with 1 ml aliquots of *Streptomyces* grown for 24 h in 50 ml of BSM containing 0.6% (wt/vol) yeast extract. Softwood lignocellulose was extracted with an ethanol-toluene solution for 8 hrs in the Soxhlet extraction apparatus as described [41]. Cultures were incubated for up to 3 weeks with shaking at 180 rpm at 37°C.

Component analysis of the biomass

Component analysis of the biomass was conducted to determine total lignin and monosugar content of the biomass. Dried softwood was ground and sieved through size 60 mesh sieving screens. Samples were prepared and characterized by the two-stage acid hydrolysis method described in Standard Biomass Analytical Procedures (NREL) [TAPPI test method (T22-om88)]. The sugars in the aqueous phase were quantified by ion chromatography using an ion exchange chromatography column (Dionex ICS-3000 DC IC) equipped with an electrochemical detector. Acid-soluble lignin was determined by UV absorbance at 205 nm with an extinction coefficient of 110 L $g^{-1}cm^{-1}$ [42].

Degradation by-products recovery and GC/MS

After submerged fermentation, samples were centrifuged at 5000 g for 10 min, filtered (Whatman no. 1), acidified to pH 1.5 with 12 M HCl and then recentrifuged to separate precipitate from the supernatant. Precipitates were washed twice with acidified water and freeze-dried. The supernatant was extracted twice with ethyl acetate and evaporated to dryness. The extracted residues were then derivatized by incubation with silanizing reagent (HMDS:TMCS:pyridine 3:1:9 (v/v/v)) at room temperature overnight to form trimethyl silyl (TMS) derivatives before analysis by GC-MS. The detection and identification of chemical compounds were performed using an Agilent 6890N Gas Chromatograph coupled with an Agilent Technologies Inert XL Mass Spectrometry Detector connected to a capillary column (Agilent HP-5 MS, HP19091S-433). Sample (1 µl) was injected into the injection port set at 200°C with a split ratio of 10:1. The column was operated in a constant flow mode using 1 ml min^{-1} of helium as a carrier gas. The mass spectrometer was operated at the electron ionization mode and scanned from 28 to 400 amu. Identification of each compound was based on retention times and matching the mass spectrum recorded with those in the spectral library (NIST/EPA/NIH Mass Spectral Library Version 2.0d, FairCom Corporation). Each determination was carried out in duplicate.

Pyrolysis GC-MS

To analyze the compositional changes, samples were subjected to the pyrolysis GC-MS (Py-GC-MS). The pyrolysis process was carried out with a CDS pyroprobe 5000 connected to a Thermo Trace GC 6890N/MSD 5975B gas chromatography/mass spectrometry system (Agilent Technologies, Inc., Bellevue, WA, USA). Samples were loaded into a quartz tube and gently packed with quartz wool prior to pyrolysis. The samples were kept briefly in the oven (210°C) for 1 min to ensure adequate removal of oxygen prior to pyrolysis and were pyrolyzed by heating instantaneously to 600oC for 1.0 min. The inlet temperature was maintained at 250°C. The resulting pyrolysis vapors were separated by means of a 30 m × 0.25 mm inner diameter (5%-phenyl)-methylpolysiloxane non-polar column, with a split ratio of 50:1. The gas flow rate was 1 ml min^{-1}. Linear heating (3°C min^{-1}) from 40 to 280°C was designated for the oven program, and to ensure that no residuals were retained, the oven was held at 280°C for 10 min after the experimental run. Identification of each compound was based on retention times and matching the mass spectrum recorded with those in the spectral library (NIST/EPA/NIH Mass Spectral Library Version 2.0d, FairCom Corporation).

Fourier transform infrared spectroscopy analysis

FTIR analysis was conducted to determine structural changes occurring on the functional groups of various components in the biomass [43-45]. ATR-FTIR spectra were recorded across the wavenumber range 4500-800 cm^{-1} with a SHIMADZU IRPrestige-21 Fourier transform infrared Spectrophotometer (Shimadzu Corp., Japan). The PIKE Technologies MIRacle ATR accessory with a high-pressure clamp (Vendor, Japan) was used. Spectra were obtained using the triangular apodization, a resolution of 4 cm^{-1} and an interval of 1 cm^{-1}. Sixty four scans were conducted for each background and sample spectra. Baseline and ATR corrections for penetration depth and frequency variations were applied using the Shimadzu IR solution 1.30 software supplied with the instrument.

Results and discussion

Analysis of the microbial community by fluorescence in situ hybridization (FISH)

The use of fluorescence-labeled oligonucleotide probes EUB 338 and ARC 915 to detect the distribution of microbial colonization in midgut indicated a wide of bacteria and archaea in the termite midgut region (Figure 1). In the termite gut, the peritrophic membrane physiologically compartmentalizes the midgut into endo and ectoperitrophic spaces (Figure 1A and 1D) and prevents microorganism invasion and injuries (mechanical or chemical) [46-48]. Interestingly, we detected strong fluorescent signals of archaea and bacteria in the front of the endoperitrophic space in the longitudinal sectioned samples, (Figure 1B-1D), while some signal representing bacteria were found in both the ectoperitrophic space and the midgut epithelium (Figure 1B and 1D). Previous ultramorphological studies demonstrated the existence of bacteria in the ectoperitrophic space of the midgut from the lower termites *Reticulitermes flavipes* and *Coptotermes formosanus [49]*. Our study further showed the bacterial population living in the midgut, including endoperitrophic spaces, ectoperitrophic spaces and midgut epithelium.

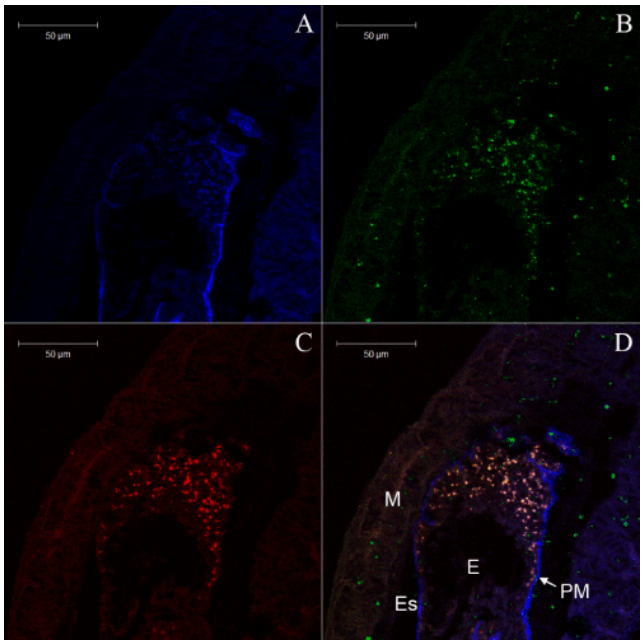

Figure 1: Confocal laser scanning microscopy of FISH after wood feeding. (A) The blue signal shows the autofluorescence in the termite gut. (B) The green signal shows the excitation of Eub 338 which was used as a probe for the detection of bacteria. (C) The red signal shows the excitation of Arc 915 which was used as a probe for the detection of archaea. (D) The overlap of A, B and C. M, Midgut wall; PM, peritrophic membrane; E, endoperitrophic space; Es, ectoperitrophic space.

Symbiotic bacteria associated with the ectoperitrophic space and epithelium in the midgut of insects is considered uncommon, not only because of the protective ability of the peritrophic membrane, but also due to the enzymes/chemicals present in this region that could reduce their ability to survive. These microorganisms might be responsible for supplementing nutrients for these insects, producing amino acids from nitrates and carbohydrates [50]. The presence of microorganisms in the midgut, especially in the ectoperitrophic space and midgut epithelium, suggests their participation in food digestion as symbiotic organisms, representing a new localizing strategy and a new possibility for exploiting food sources found in the environment. However, how bacteria bridge the peritrophic membrane is still not clear.

Isolation, screening and identification of microorganisms

Of the 100 initial strains, only two strains, B207 and L201, oxidized guaiacol and decolorized azure B. The results of guaiacol oxidation and azure B decolorization for the strains B207 and L201 are shown in Figure 2. Guaiacol was oxidized by the two strains first (7 days) after which the dyes were decolorized (14 days), which demonstrated that guaiacol could be employed as the expeditious indicator for lignin degradation.

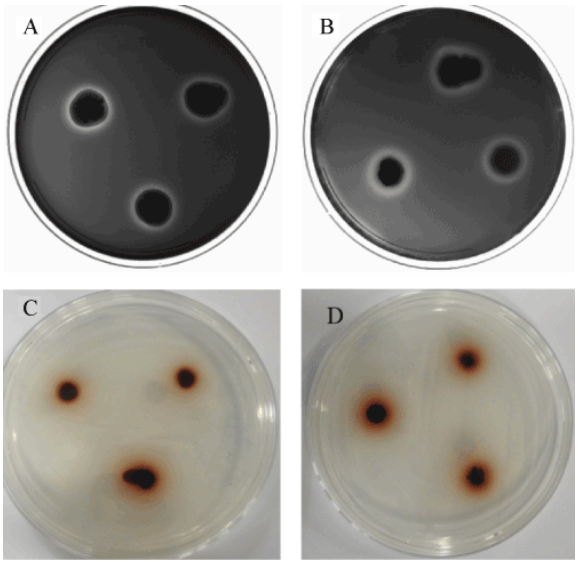

Figure 2: Plates screened for color changes caused by positive lignin-degrading strains. Colonies of B207 (A) and L201 (B) grown on PDA medium containing 0.01% azure B were incubated for 14 days at 28°C, while colonies of B207 (C) and L201 (D) grown on PDA medium containing 0.01% guaiacol were incubated for 7 days at 28°C.

Based on their 16S rDNA gene sequences, the strains B207 and L201 had the highest similarities to *streptomyces sanglieri* (99.378%) and *streptomyces atratus* (99.378%). The phylogenetic relationship of strains B207 and L201 to other organisms included in family *Streptomycetaceae* suggested that strains B207 and L201 were members of the genus streptomyces (Figure 3). Previously, streptomycetes have been isolated from the guts of termites and other wood feeding insects, which provides further evidence that these microbes could be an integral part of the lignocellulosic digestion in the wood feeding termite [51-53].

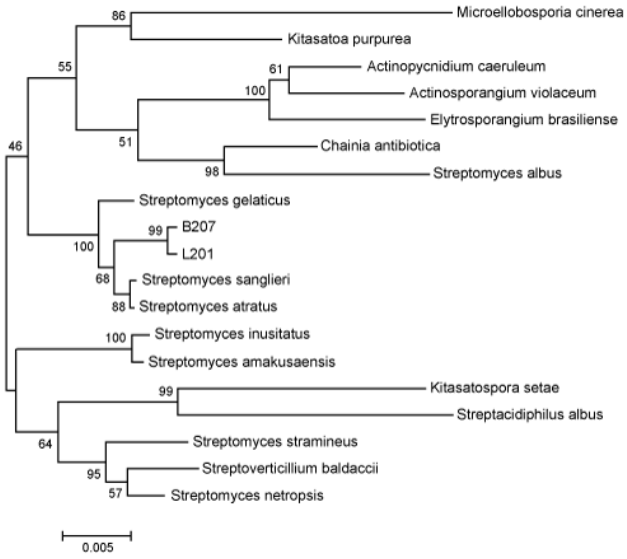

Figure 3: Phylogenetic tree showing the relationship of strains B207 and L201 to other organisms on the basis of 16S rDNA sequences. The tree was constructed with the neighbor-joining method using 1000 bootstrap replicates. The scale bar represents 0.005 substitutions per nucleotide position. Numbers mark the bootstrap values for each node out of 100 bootstrap resampling.

FTIR analysis

The FTIR spectrum shows the effects of isolated bacteria digestion on the functional chemical groups of softwood biomass (Figure 4). The assignments of major peaks are listed in Table 1. Compared to the untreated wood, the biologically treated wood showed significant changes in the region 1800-800 cm^{-1}. The peak 1738/1734 cm^{-1} has been assigned to the carbonyl stretching vibration in acetyl groups on hemicelluloses [45]. Since acetyl groups are bound through an ester linkage to hemicellulose chains, the intensity disappearance at 1738/1734 cm^{-1} revealed decomposition and/or rearrangement of hemicellulose by B207 and L201, which may relax and simplify the structural integrity and complexity of softwood [8]. The peak appearing at 1655 cm^{-1} represents carbonyl stretching in conjugated ρ-substituted aryl ketones and it was found to be notably decreased in inoculated samples. This could be attributed to the deformation of the carbonyl existing in the side chains of the softwood lignin structural units and/or modification of aldehyde groups lying in C-γ or keto groups lying in C-β regions [14]. Meanwhile, the spectral decrease at 1593 cm^{-1}, 1268 cm^{-1}, and 1240 cm^{-1} corresponds to aromatic skeletal guaiacyl unit vibrations in the treated samples. Thus, it is clear that this bacterially treated wood showed removal and/or modification of lignin functional groups. Similarly, the signal vibrations at bands 1050 cm^{-1}, 1035 cm^{-1}, 1372 cm^{-1}, and 896 cm^{-1} represent crystalline structure changes in cellulose. On the other hand, cellulose content increased in treated samples according to the results of chemical component analysis (Table 2), and the content ratio of lignin to cellulose decreased by 12% after degradation by the bacteria B207 and L201. Through FTIR analysis, the B207 and L201 treated wood displayed significant differences in the functional group regions of lignin and hemicellulose, which indicates decomposition and/or rearrangement of lignocellulosic biomass. As is well known, the removal of hemicellulose and lignin will enhance the enzymatic hydrolysis efficiency of cellulose [3,54,55]. Therefore, the role of bacteria may involve the initialized decomposition of lignocellulose and benefit the further conversion of cellulose in termite.

Wavenumber (cm^{-1})	Assignment	Band numbers
1738/1734	C=O stretching vibration in acetyl groups on hemicelluloses	1
1655	C=O stretch in conjugated carbonyl groups	2
1593	Aromatic skeletal vibration plus C=O stretch	3
1372	Aliphatic C-H stretch in CH3	4
1268	Guaiacyl ring breathing, C-O stretch in lignin and C-O linkage in guiacyl aromatic methoxyl groups	5
1240	Syringyl ring and C-O stretching vibration in lignin, xylan and ester groups	6
1050	C-O stretch in cellulose and hemicellulose	7
1035	C-O deformations in primary alcohols, aromatic C-H in-plane deformation	8
896	C-H deformation vibration in cellulose	9

Table 1: FTIR bands that have been assigned to different wood components. Numbers in the table refer to the numbers assigned to the bands in Figure 4.

Samples	Control	B207	L201
Arabinan	0.74 ± 0.05	0.61 ± 0.07	0.62 ± 0.06

Galactan	1.40 ± 0.03	1.39 ± 0.02	1.39 ± 0.05
Glucan	38.88 ± 0.43	43.62 ± 0.60	43.37 ± 0.87
Mannan/xylan	5.84 ± 0.10	6.19 ± 0.22	6.24 ± 0.16
Acid soluble lignin	0.90 ± 0.01	0.73 ± 0.02	0.75 ± 0.001
Acid insoluble lignin	28.21 ± 0.30	28.03 ± 0.14	27.94 ± 0.35
Ash	0.55 ± 0.14	0.71 ± 0.14	0.58 ± 0.39

Table-2: Compositional analysis (wt% dry) of untreated softwood control and softwood samples treated by B207 and L201, respectively.

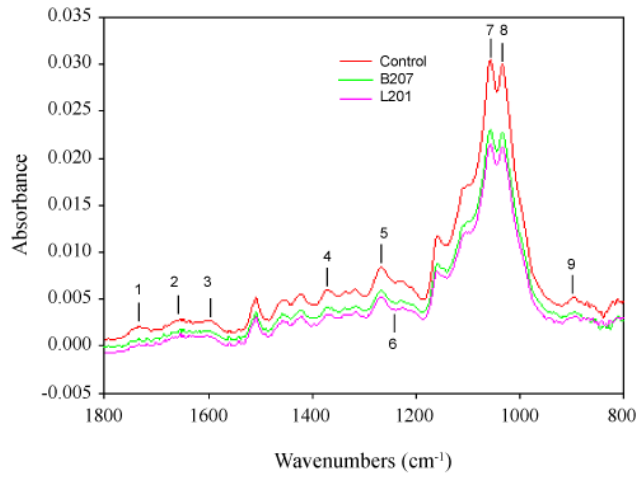

Figure 4: FTIR spectrum of untreated softwood control (red line) and softwood samples treated by B207 (green line) and L201 (pink line), respectively. The band assignments refer to Table 1.

Py-GC/MS and GC/MS analysis

Py-GC/MS was applied to further analyze the lignin composition changes of bio-treated softwood samples by B207 and L201. Total ion current (TIC) data from Py-GC/MS of softwood at 600°C were collected and selected pyrolysis products are listed in Table 3. In order to increase the sensitivity of the quantitation method, the peak areas were integrated using ion specific m/z. Ions used for the integration are presented in Table 3. The peak area of carbon dioxide was considered as 100% in order to normalize other components present and to characterize the composition changes of the samples. The main pyrolyzates derived from hydroxyphenyl-(H) and guaiacyl-(G) phenylpropanoid include: toluene, benzylmethylketone, phenol, 3-methylphenol, 2-methoxyphenol, naphthalene, 2-methoxy-4-methylphenol, 2-methoxy-4-vinylphenol, trans-2-methoxy-4-(1-propenyl) phenol, and vanillin. Furthermore, distribution differences for the H and G units were found in softwood residues between treated and untreated samples. Compared with untreated sample (62.9%), the G content of B207 and L201 treated softwood was reduced to (59.78%) and (58.99%) respectively. The areas of pyrogram peaks, typical for the hydroxyphenyl- and guaiacyl-type degradation products, were summed and normalized to 100% in order to determine quantitative changes in the chemical structure of the lignin components. Consequently, the total G/H ratio was changed from 6.12 to 3.33 and 4.48, respectively (Figure 5). The preferential degradation of G units by strains B207 and L201 may have resulted from lignin peroxidase (LiP) activity, which is produced by fungi and actinomycetes, and can catalyze lignin breakdown. Ramachandra et al. (1988) described a special Lip ALip-P3 from *Streptomyces viridosporus* T7A [56]. The LiP was able to degrade guaiacyl (G) and syringyl (S) structures in non-phenolic methylated lignin [57] which was differentiated from other ligninolytic enzymes: namely, manganese peroxidase (MnP) and laccase. The breakdown of C_{α}-C_{β} and/or β-O-4 on lignin side chain will produce soluble lignin derivatives. Crawford et al. (1983) reported that lignocellulose degradation by *Streptomyces viridosporus* caused lignin depolymerization and production of a water-soluble lignin polymer, an acid precipitable polymeric lignin (APPL) [58]. To track degraded lignin compounds, APPL products were also determined in the supernatant from untreated and treated samples. After bacterial growth on softwood lignocellulose for 3 weeks, culture supernatants were acidified and centrifuged. Pyrolysis products derived from the acid precipitates of treated and untreated softwood are shown in Table 4. The results show evident increase in the concentration of single-ring aromatic compounds in degraded softwood samples. Compared to control, the total lignin ratio was increased from 1.01 to 2.99 and 2.75. In the control sample, the pyrolyzates only contained carbon dioxide, and a very small proportion of benzene. However, the softwood inoculated with strain B207 and L201 caused a very different distribution of compounds in the pyrogram. The main components in APPL were found to be toluene, pentenol, benzene, phenol, and 4-methylphenol. Phenolic compound found in the precipitates were probably due to degradation of aryl-ether linkages, which are known to be major inter-unit linkages in lignin polymerization [59]. The appearance of these compounds in APPL confirms the depolymerization/modification of the lignin moiety.

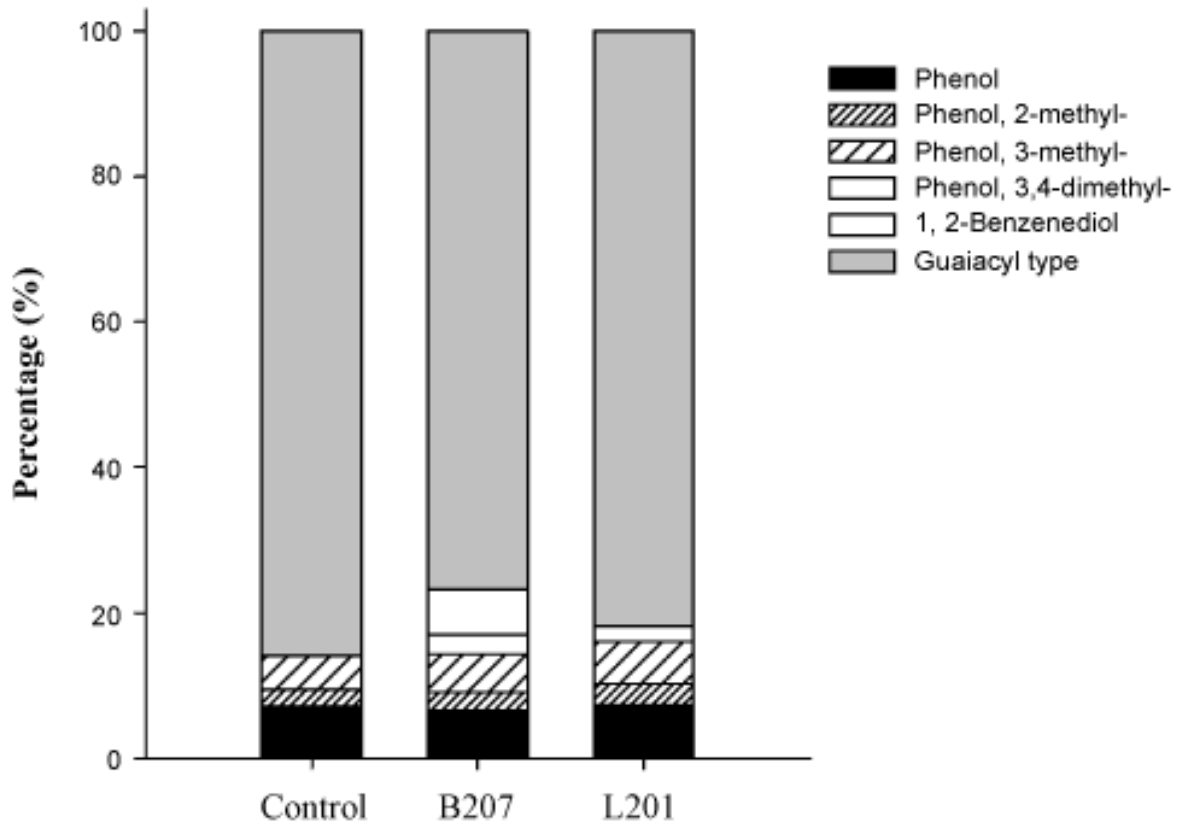

Figure 5: Distribution (after normalization to 100%) of the hydroxyphenyl- type and guaiacyl-type degradation products from pyrolysis of untreated softwood control and softwood samples treated by B207 and L201, respectively. Hydroxyphenyl-type: phenol; phenol, 2-methyl-; phenol, 3-methyl-; phenol, 3,4-dimethyl-; 1,2-benzenediol.

Compound	Source[a]	Formula	MW[b]	RT (min)	Ions used for integration	Control Area (%)	B207 Area (%)	L201 Area (%)
Carbon dioxide		CO_2	44	1.619	44,34,32	100	100	100
Toluene	L	C_7H_8	92	4.096	91,92,57	14.05	13.61	12.69
Benzyl methyl ketone	L	$C_9H_{10}O$	134	4.121	43,91,92	8.48	6.58	4.73
Ethylbenzene	L	C_8H_{10}	106	5.899	106,91,43		1.05	1.23
Styrene	L	C_8H_8	104	6.576	104,103,78	4.1	3.95	2.88
Phenol	L,H	C_6H_6O	94	8.924	94,66,65	7.78	7.49	6.13
1,2-Cyclopentanedione, 3-methyl-		$C_6H_8O_2$	112	9.986	112,69,55		3.27	1.65
Benzene, 1-ethynyl-4-methyl-	L	C_9H_8	116	10.353	115,116,89	4.93	4.65	4.45
Phenol, 2-methyl-	L,H	C_7H_8O	108	10.718	108,107,79	2.58	2.73	2.49
Phenol, 3-methyl-	L,H	C_7H_8O	108	11.273	107,108,77	5.08	6.17	4.8
Phenol, 2-methoxy-	L,G	$C_7H_8O_2$	124	11.514	109,124,81	16.24	12.38	11.6
Phenol, 3,4-dimethyl-	L,H	$C_8H_{10}O$	122	13.017	122,107,121		3.04	1.87

Naphthalene	L	$C_{10}H_8$	128	13.818	128,127	10.89	9.64	7.91
Phenol, 2-methoxy-4-methyl-	L,G	$C_8H_{10}O_2$	138	14.047	138,123,95	9.59	8.84	6.84
1,2-Benzenediol	L,H	$C_6H_6O_2$	110	14.477	110,64,63		6.94	
Phenol, 4-ethyl-2-methoxy-	L,G	$C_9H_{12}O_2$	152	16.074	137,152,122	3.24	3.1	2.53
2-Methoxy-4-vinylphenol	L,G	$C_9H_{10}O_2$	150	16.877	150,135,107	22.19	19.3	15.96
Eugenol	L,G	$C_{10}H_{12}O_2$	164	17.83	164,149,131	3.32	3.44	1.46
Vanillin	L,G	$C_8H_8O_3$	152	18.828	151,152,81	6.93	7.42	4.98
Phenol, 2-methoxy-4-(1-propenyl)-	L,G	$C_{10}H_{12}O_2$	164	18.93	164,149,77	1.68	1.72	1.03
Phenol, 2-methoxy-4-(1-propenyl)-, (E)-	L,G	$C_{10}H_{12}O_2$	164	19.81	164,149,152	13.65	13.48	12.4
Phenol, 2-methoxy-4-propyl-	L,G	$C_{10}H_{14}O_2$	166	20.013	137,166,60	1.21	1.63	1.14
Ethanone, 1-(4-hydroxy-3-methoxyphenyl)-	L,G	$C_9H_{10}O_3$	166	20.651	151,166,123	3.82	4.87	3.05
2-Propanone, 1-(4-hydroxy-3-	L,G	$C_{10}H_{12}O_3$	180	21.537	137,180,122	3.44	2.59	2.22
methoxyphenyl)-								
Vanilacetic acid	L,G	$C_9H_{10}O_4$	182	23.805	137,182,138	5.43	4.75	2.11
(E)-Conipheryl alcohol	L,G	$C_{10}H_{12}O_3$	180	24.265	137,180,124	0.78	1.19	1.57
4-Hydroxy-2-methoxycinnamaldehyde	L,G	$C_{10}H_{10}O_3$	178	25.416	178,135,147	3.08	3.54	1.63
Phenanthrene	L	$C_{14}H_{10}$	178	26.146	178,176,179	2	1.78	1.32
	H/L (%)					10.27	17.96	13.16
	G/L (%)					62.9	59.78	58.99
	G/H ratio					6.12	3.33	4.48

Table-3: Principal pyrolysis products of untreated softwood control and softwood samples treated by B207 and L201, respectively.

[a] L, Lignin; G, guaiacyl type; H, hydroxyphenyl type

[b] Molecular weight

Compound	**Origin[a]**	**Formula**	**MW[b]**	**RT (min)**	**Ions used for integration**	**Control Area (%)**	**B207 Area (%)**	**L201 Area (%)**
Carbon dioxide		CO_2	44	1.615	44,34,32	100	100	100
Pentenol		$C_5H_{10}O$	86	1.897	41,40,39		24.16	26.94
Propanal, 2-methyl-		C_4H_8O	72	2.066	41,43,72		6.63	5.41
Furan, 2-methyl-		C_5H_6O	82	2.299	82,53,81		6.67	10.41
Butanal, 3-methyl-		$C_5H_{10}O$	86	2.664	41,44,43		2.25	1.86
Benzene	L	C_6H_6	78	2.767	78,77,41	1.31	16.25	10.66
Toluene	L	C_7H_8	92	4.082	91,92,65		56.3	46.15
p-Xylene	L	C_8H_{10}	106	6.087	91,106,105		6.36	3.34
Styrene	L	C_8H_8	104	6.577	104,103,78		6.23	4.78
Benzene, 1-ethyl-3-methyl-	L	C_9H_{12}	120	8.305	105,120,106		0.92	1.21
Phenol	L,H	C_6H_6O	94	8.921	94,103,66		12.47	9.97

Benzene, 1-propenyl-	L	C_9H_{10}	118	9.18	118,117,115		1.25	1.15
4-Methylphenol	L,H	C_7H_8O	108	11.248	107,108,77		19.73	15.2
Phenol, 2-methoxy-	L,G	$C_7H_8O_2$	124	11.519	109,124,81		6.47	3.64
Benzyl nitrile		C_8H_7N	117	12.766	117,90,116		3.78	3.26
Naphthalene	L	$C_{10}H_8$	128	13.818	128,129,127		4.39	2.03
Phenol, 2-methoxy-4-methyl-	L,G	$C_8H_{10}O_2$	138	14.045	138,123,95		3.59	1.32
Benzenepropanenitrile		C_9H_9N	131	15.203	91,131,65		2.88	3.2
Indolizine		C_8H_7N	117	16.485	117,90,89		8.47	6.15
Squalane		$C_{30}H_{62}$	422	38.72	57,71,85		5.85	9.9
Acetic acid, 3,7,11,15-tetramethyl-hexadecyl ester		$C_{22}H_{44}O_2$	340	39.05	57,69,83		3.15	5.58
9-Hexadecen-1-ol, (Z)-		$C_{16}H_{32}O$	240	39.38	69,55,83		1.6	2.89
Total lignin content (%)						1.3	42.67	34.42

Table 4: Principal pyrolysis products of APPL and area ratio

[a] L, Lignin; G, guaiacyl type; H, hydroxyphenyl type

[b] Molecular weight

Additionally, we have determined the small fragment accumulation in acidified culture supernatants. Ethyl acetate extracted compounds were analyzed through GC/MS. Table 5 shows the patterns of ethyl acetate extracted compounds from the culture supernatants. Both inoculated and uninoculated control supernatants contained significant amounts of these compounds, but with different fragment patterns. In the control, almost all the fragments were derived from carbohydrates compounds, such as lactic acid, succinic acid and pyroglutamic acid, but were almost totally absent in the inoculated supernatants due to utilization as carbon source by streptomyces. In contrast, oxalic acid, propanedioic acid, and glutaric acid increased 10 fold or appeared as principal components in the inoculated samples. Oxalic acid is secreted by wood-degrading fungi, and it is thought to depolymerize cellulose and hemicellulose through non-enzymatic mechanisms. As such it has been proven to be a strong catalyst for hemicellulose hydrolysis [60], which is consistent with our FTIR results and component analysis. Furthermore, lignin-derived compounds were also found in the culture supernatants. The principal substituted phenolic acids that would be expected to arise from streptomyces attack on hydroxyphenyl- and guaiacyl propane units in lignin include 2-hydroxyphenylacetic acid, 4-hydroxybenzoic acid, vanillic acid, 4-hydroxyphenylacetic acid, 2-hydroxy-3-(4-hydroxyphenyl) propanoic acid, and ferulic acid. Substituted benzoic acids 4-hydroxybenzoic acid and vanillic acid have been reported as lignin degradation intermediates in fungi [61]. The accumulation of benzoic acid and vanillic acid is derived from the cleavage of C_α and C_β of the aliphatic side chain in the G unit [62]. The appearance of ferulic acid, found to be linked at different positions on the arabinose residues in the arabinoxylans through ester bonds [63], indicated hydrolysis of these ester bonds, which are considered to be critical to hemicellulose degradation; the hydrolysis of which was also supported by the FTIR results. The presence of low-molecular-weight aromatics in the controls was probably due to leaching over the extended incubation period. Overall, Py-GC/MS and GC/MS revealed that the strains B207 and L207, isolated from the midgut of termites, deconstructed softwood through degradation of hemicellulose and conversion of the condensed G unit into soluble lignin derivatives.

Compound	**Source**[a]	**Formula**	**MW**[b]	**RT_c (min)**	**Ions used ford integration**	**Control Area (%)**	**B207 Area (%)**	**L201 Area (%)**
Butyl acetate		$C_6H_{12}O_2$	116	5.801	43,56,73		3.38	2.9
Isobutyric acid		$C_4H_8O_2$	88	7.987	73,75,145	0.93		
Isovaleric acid		$C_5H_{10}O_2$	102	9.845	75,73,159	0.63		
Lactic acid		$C_3H_6O_3$	90	15.885	73, 147, 117	23.54		
Glycolic acid		$C_2H_4O_3$	76	16.476	73,147,66	1.48		
2-Furoic acid		$C_5H_4O_3$	112	18.945	125,169,95		2.87	2.87
Oxalic acid		$C_2H_2O_4$	90	19.367	73,147,45	1.52	12.14	8.57

2-Hydroxy-3-methylbutyric acid		$C_5H_{10}O_3$	118	20.662	73,145,147	2.64		0.7
Propanedioic acid		$C_3H_4O_4$	104	22.548	147,73,75		4.61	4.13
3-Hydroxyisovaleric acid		$C_5H_{10}O_3$	118	22.644	131,73,147		1.13	1.04
Benzoic acid	L	$C_7H_6O_2$	122	23.907	105,179,77	0.31	3.68	3.23
2-hydroxy-4-methylpentanoic acid		$C_6H_{12}O_3$	132	24.001	73,159,103	0.7		1.72
Succinic Acid		$C_4H_6O_4$	118	27.344	147,73,75	47.89	1.09	0.84
2,3-dihydroxy-2-methyl-propanoic acid		$C_4H_8O_4$	120	27.888	73,219,147	1.17	2.84	3.62
Fumaric acid		$C_4H_4O_4$	116	28.783	245,73,147	1.44		
Citraconic acid		$C_5H_6O_4$	130	28.998	147,73,45			2.02
Glutaric acid		$C_5H_8O_4$	132	31.274	73,147,75	0.54	12.16	9.57
4-Hydroxyvaleric acid		$C_5H_{10}O_3$	118	32.971	73,117,147	0.76		2.76
Malic acid		$C_4H_6O_5$	134	35.106	73,147,233	5.53		
trans-3-Hexenedioic acid		$C_6H_8O_4$	144	35.343	73,147,75		2.63	2.54
Pyroglutamic acid		$C_5H_7NO_3$	129	35.983	156,73,147	10.42		
2-Hydroxyphenylacetic acid	L,H	$C_8H_8O_3$	152	37.68	73,147,253		6.94	8.18
Pimelic acid		$C_7H_{12}O_4$	160	39.096	73,75,55		1.27	1.23
4-hydroxybenzoic acid	L,H	$C_7H_6O_3$	138	39.798	73,267,193	0.68	6.31	4.71
4-hydroxyphenylacetic acid	L,H	$C_8H_8O_3$	152	40.335	73,179,75	0.42	10.91	8.43
Suberic acid		$C_8H_{14}O_4$	174	42.562	73,75,303		3.4	3.92
Vanillic acid	L,G	$C_8H_8O_4$	168	44.874	297,73,312	2.04	9.59	8.36
Azelaic acid		$C_9H_{14}O_4$	188	45.991	73,75,55	0.51	3.34	2.54
2-Hydroxy-3-(4-hydroxyphenyl) propanoic acid	L,H	$C_9H_{10}O_4$	182	49.687	73,179,147		1.13	1.64
Ferulic acid	L,G	$C_{10}H_{12}O_4$	196	52.983	209,73,340		1.92	1.88
Total lignin content (%)						1.31	11.37	9.92

Table 5: Results obtained from GC-MS analysis of the derivatized extracts from untreated softwood control and softwood samples treated by B207 and L201, respectively.

[a] L, Lignin; G, guaiacyl type; H, hydroxyphenyl type

[b] Molecular weight

[c] Retention times of TMS derivatives

[d] Ions of TMS derivative

Conclusion

In this study we confirmed the existence of microflora in the termite midgut, and provided a clear microbial distribution of the bacteria and archaea. Two streptomyces sp. strains were isolated, providing more accurate information about the location of streptomyces in the termite gut. In addition, biological pretreatment of softwood by the two isolated streptomyces strains significantly changed lignin structure, especially caused G unit degradation. It is therefore probable that during the pretreatment process, and prior to biomass reaching the termite hindgut, colonized microbes play a synergistic role with the termite in the wood digestion process.

Acknowledgements

The authors would like to thank Dr. Christine Davitt for excellent technical assistance, Jie Feng for sequencing analysis (Johns Hopkins University), and Dr. Jim O'Fallon for manuscript editing. This work was financially supported by the Agriculture Research Center, Washington State University.

References

1. Arakawa G, Watanabe H, Yamasaki H, Maekawa H, Tokuda G (2009) Purification and molecular cloning of xylanases from the wood-feeding termite, Coptotermes formosanus Shiraki. Biosci Biotechnol Biochem 73: 710-718.
2. Scharf ME, Tartar A (2008) Termite digestomes as sources for novel lignocellulases. Biofuels, Bioproducts and Biorefining 2: 540-552.
3. Yang B, Wyman CE (2004) Effect of xylan and lignin removal by batch and flowthrough pretreatment on the enzymatic digestibility of corn stover cellulose. Biotechnol Bioeng 86: 88-98.
4. Ohgren K, Bura R, Saddler J, Zacchi G (2007) Effect of hemicellulose and lignin removal on enzymatic hydrolysis of steam pretreated corn stover. Bioresour Technol 98: 2503-2510.
5. Breznak JA, Brune A (1994) Role of Microorganisms in the Digestion of Lignocellulose by Termites. Ann Rev Entomol 39: 453-487.
6. Wong D (2009) Structure and Action Mechanism of Ligninolytic Enzymes. Appl Biochem Biotechnol 157: 174-209.
7. Anderson W, Akin D (2008) Structural and chemical properties of grass lignocelluloses related to conversion for biofuels. J Ind Microbiol Biotechnol 35: 355-366.
8. Harmsen P, Huijgen W, Bermudez L, Bakker R (2010) Literature review of physical and chemical pretreatment processes for lignocellulosic biomass. Wageningen: Wageningen UR, Food & Biobased Research.
9. Hendriks ATWM, Zeeman G (2009) Pretreatments to enhance the digestibility of lignocellulosic biomass. Bioresour Technol 100: 10-18.
10. Taherzadeh MJ, Karimi K (2008) Pretreatment of lignocellulosic wastes to improve ethanol and biogas production: a review. Int J Mol Sci 9: 1621-1651.
11. Hatakka AI (1983) Pretreatment of wheat straw by white-rot fungi for enzymic saccharification of cellulose. Appl Microbiol Biotechnol 18: 350-357.
12. Lee JW, Gwak KS, Park JY, Park MJ, Choi DH, et al. (2007) Biological pretreatment of softwood Pinus densiflora by three white rot fungi. J Microbiol 45: 485-491.
13. Dey S, Maiti TK, Bhattacharyya BC (1994) Production of some extracellular enzymes by a lignin peroxidase-producing brown rot fungus, Polyporus ostreiformis, and its comparative abilities for lignin degradation and dye decolorization. Appl Environ Microbiol 60: 4216-4218.
14. Singh D, Zeng J, Laskar DD, Deobald L, Hiscox WC, et al. (2011) Investigation of wheat straw biodegradation by Phanerochaete chrysosporium. Biomass and Bioenergy 35: 1030-1040.
15. Zeng J, Singh D, Chen S (2011) Biological pretreatment of wheat straw by Phanerochaete chrysosporium supplemented with inorganic salts. Bioresour Technol 102: 3206-3214.
16. Brune A (2007) Microbiology: woodworker's digest. Nature 450: 487-488.
17. Ke J, Sun JZ, Nguyen HD, Singh D, Lee KC, et al. (2010) In-situ oxygen profiling and lignin modification in guts of wood-feeding termites. Insect Science 17: 277-290.
18. Ohkuma M (2003) Termite symbiotic systems: efficient bio-recycling of lignocellulose. Appl Microbiol Biotechnol 61: 1-9.
19. Chaffron S, von Mering C (2007) Termites in the woodwork. Genome Biol 8: 229.
20. Chandrasekharaiah M, Thulasi A, Bagath M, Kumar DP, Santosh SS, et al. (2011) Molecular cloning, expression and characterization of a novel feruloyl esterase enzyme from the symbionts of termite(Coptotermes formosanus) gut. BMB Rep 44: 52-57.
21. Lo N, Tokuda G, Watanabe H (2011) Evolution and Function of Endogenous Termite Cellulases: Biology of Termites: a Modern Synthesis. (Bignell DE, Roisin Y, Lo N edn), Springer, Netherlands, 51-67.
22. Zhang D, Lax AR, Bland JM, Allen AB (2011) Characterization of a new endogenous endo-[beta]-1,4-glucanase of Formosan subterranean termite (Coptotermes formosanus). Insect Biochem Mol Biol 41: 211-218.
23. Hongoh Y, Ohkuma M, Kudo T (2003) Molecular analysis of bacterial microbiota in the gut of the termite Reticulitermes speratus (Isoptera; Rhinotermitidae). FEMS Microbiol Ecol 44: 231-242.
24. Watanabe H, Nakamura M, Tokuda G, Yamaoka I, Scrivener AM, et al. (1997) Site of secretion and properties of endogenous endo-beta-1,4-glucanase components from Reticulitermes speratus (Kolbe), a Japanese subterranean termite. Insect Biochem Mol Biol 27: 305-313.
25. Yang H, Peng JX, Liu KY, Hong HZ (2006) Diversity and function of symbiotic microbes in the gut of lower termites. Wei Sheng Wu Xue Bao 46: 496-499.
26. Kudo T (2009) Termite-microbe symbiotic system and its efficient degradation of lignocellulose. Biosci Biotechnol Biochem 73: 2561-2567.
27. Warnecke F, Luginbuhl P, Ivanova N, Ghassemian M, Richardson TH, et al. (2007) Metagenomic and functional analysis of hindgut microbiota of a wood-feeding higher termite. Nature 450: 560-565.
28. Tartar A, Wheeler MM, Zhou X, Coy MR, Boucias DG, et al. (2009) Parallel metatranscriptome analyses of host and symbiont gene expression in the gut of the termite Reticulitermes flavipes. Biotechnol Biofuels 2: 25.
29. Geib SM, Filley TR, Hatcher PG, Hoover K, Carlson JE, et al. (2008) Lignin degradation in wood-feeding insects. Proc Natl Acad Sci 105: 12932.
30. Coy MR, Salem TZ, Denton JS, Kovaleva ES, Liu Z, et al. (2010) Phenol-oxidizing laccases from the termite gut. Insect Biochem Mol Biol 40: 723-732.
31. Tokuda G, Yamaoka I, Noda H (2000) Localization of Symbiotic Clostridia in the Mixed Segment of the Termite Nasutitermes takasagoensis (Shiraki). Appl Environ Microbiol 66: 2199-2207.
32. Kikuchi Y, Meng XY, Fukatsu T (2005) Gut symbiotic bacteria of the genus Burkholderia in the broad-headed bugs Riptortus clavatus and Leptocorisa chinensis (Heteroptera: Alydidae). Appl Environ Microbiol 71: 4035.
33. Yanagita K, Manome A, Meng XY, Hanada S, Kanagawa T, et al. (2003) Flow cytometric sorting, phylogenetic analysis and in situ detection of Oscillospira guillermondii, a large, morphologically conspicuous but uncultured ruminal bacterium. Int J Syst Evol Microbiol 53: 1609-1614.
34. Cho MJ, Kim YH, Shin K, Kim YK, Kim YS, et al. Symbiotic adaptation of bacteria in the gut of Reticulitermes speratus: Low endo-[beta]-1, 4-glucanase activity. Biochem Biophys Res Commun 395: 432-435.
35. Okino L, Machado K, Fabris C, Bononi V (2000) Ligninolytic activity of tropical rainforest basidiomycetes. World J Microbiol Biotechnol 16: 889-893.
36. Archibald FS (1992) A new assay for lignin-type peroxidases employing the dye azure B. Appl Environ Microbiol 58: 3110-3116.
37. Arora DS, Gill PK (2001) Comparison of two assay procedures for lignin peroxidase. Enzyme Microb Technol 28: 602-605.
38. Morisaki K, Fushimi T, Kaneko S, Kusakabe I, Kobayashi H (2001) Screening for phenoloxidases from edible mushrooms. Biosci Biotechnol Biochem 65: 2334-2336.
39. Mercer DK, Iqbal M, Miller P, McCarthy AJ (1996) Screening actinomycetes for extracellular peroxidase activity. Appl Environ Microbiol 62: 2186-2190.
40. Altschul SF, Madden TL, Schäffer AA, Zhang J, Zhang Z, et al. (1997) Gapped BLAST and PSI-BLAST: a new generation of protein database search programs. Nucleic Acids Res 25: 3389-3402.
41. ASTM (1996) Standard Test Method for Ethanol-Toluene Solubility of Wood.
42. Zimbardi F, Viggiano D, Nanna F, Demichele M, Cuna D, et al. (1999) Steam explosion of straw in batch and continuous systems. Appl Biochem Biotechnol 77: 117-125.
43. Labbe N, Rials TG, Kelley SS, Cheng ZM, Kim JY, et al. (2005) FT-IR imaging and pyrolysis-molecular beam mass spectrometry: new tools to investigate wood tissues. Wood Sci Technol 39: 61-76.

44. Oh SY, Yoo DI, Shin Y, Kim HC, Kim HY, et al. (2005) Crystalline structure analysis of cellulose treated with sodium hydroxide and carbon dioxide by means of X-ray diffraction and FTIR spectroscopy. Carbohydr Res 340: 2376-2391.
45. Pandey KK, Pitman AJ (2003) FTIR studies of the changes in wood chemistry following decay by brown-rot and white-rot fungi. Int Biodeter Biodegr 52: 151-160.
46. Terra WR, Ferreira C (1994) Insect digestive enzymes: properties, compartmentalization and function. Kidlington, ROYAUME-UNI: Elsevier.
47. Terra WR (2001) The origin and functions of the insect peritrophic membrane and peritrophic gel. Arch Insect Biochem Physiol 47: 47-61.
48. Lehane MJ, Billingsley P (1996) Biology of the insect midgut. Chapman & Hall.
49. Breznak JA, Pankratz HS (1977) In situ morphology of the gut microbiota of wood-eating termites [Reticulitermes flavipes (Kollar) and Coptotermes formosanus Shiraki]. Appl Environ Microbiol 33: 406-426.
50. Caetano FH, Bution ML, Zara FJ (2009) First report of endocytobionts in the digestive tract of ponerine ants. Micron 40: 194-197.
51. Pasti MB, Pometto AL III, Nuti MP, Crawford DL (1990) Lignin-solubilizing ability of actinomycetes isolated from termite (Termitidae) gut. Appl Environ Microbiol 56: 2213-2218.
52. Harazono K, Yamashita N, Shinzato N, Watanabe Y, Fukatsu T, et al. (2003) Isolation and characterization of aromatics-degrading microorganisms from the gut of the lower termite Coptotermes formosanus. Biosci Biotechnol Biochem 67: 889-892.
53. Watanabe Y, Shinzato N, Fukatsu T (2003) Isolation of actinomycetes from termites' guts. Biosci Biotechnol Biochem 67: 1797-1801.
54. Ohgren K, Bura R, Saddler J, Zacchi G (2007) Effect of hemicellulose and lignin removal on enzymatic hydrolysis of steam pretreated corn stover. Bioresour Technol 98: 2503-2510.
55. Pérez J, Muñoz D, de la R, Martínez J (2002) Biodegradation and biological treatments of cellulose, hemicellulose and lignin: an overview. Int Microbiol 5: 53-63.
56. Ramachandra M, Crawford DL, Hertel G (1988) Characterization of an extracellular lignin peroxidase of the lignocellulolytic actinomycete Streptomyces viridosporus. Appl Environ Microbiol 54: 3057-3063.
57. Hatakka A (2005) Biodegradation of Lignin: Wiley-VCH Verlag GmbH & Co. KGaA.
58. Crawford DL, Pometto AL III, Crawford RL (1983) Lignin Degradation by Streptomyces viridosporus: Isolation and Characterization of a New Polymeric Lignin Degradation Intermediate. Appl Environ Microbiol 45: 898-904.
59. Camarero S, Bocchini P, Galletti GC, Martínez AT (1999) Pyrolysis-gas chromatography/Mass spectrometry analysis of phenolic and etherified units in natural and industrial lignins. Rapid Commun Mass Sp 13: 630-636.
60. Lee JW, Rodrigues RCLB, Kim HJ, Choi I-G, Jeffries TW (2010) The roles of xylan and lignin in oxalic acid pretreated corncob during separate enzymatic hydrolysis and ethanol fermentation. Bioresour Technol 101: 4379-4385.
61. Kirk TK, Higuchi T, Chang H (1980) Program US-JCS Lignin biodegradation: microbiology, chemistry, and potential applications: CRC Press.
62. Hammel KE, Cullen D (2008) Role of fungal peroxidases in biological ligninolysis. Curr Opin Plant Biol 11: 349-355.
63. Hua D, Ma C, Song L, Lin S, Zhang Z, et al. (2007) Enhanced vanillin production from ferulic acid using adsorbent resin. Appl Microbiol Biotechnol 74: 783-790.